Quantifying the Benefits of Building Instruments to FEMA P-58 Rapid Post-Earthquake Damage and Loss Predictions

Gemma Cremen[a,1,*], Jack W. Baker[b,2]

[a]*Room 214, Building 540, 439 Panama Mall, Stanford, CA 94305, USA*
[b]*Room 283, Y2E2, 473 Via Ortega, Stanford, CA 94305, USA*

Abstract

Seismic instrumentation in a building is used to accurately capture its response during an earthquake, and so should enable enhanced rapid post-earthquake predictions of the event's consequences for the building (among other benefits). Such instrumentation is costly, however, thus it is useful to know the extent to which varying degrees of its implementation within a building affect the accuracy of these predictions. The purpose of this study is to develop a methodology for quantifying the errors in post-earthquake damage and loss consequence predictions calculated from the FEMA P-58 Seismic Performance Assessment procedure, when different numbers of building instruments are used to capture the response of a building in a given event. We use responses measured in instrumented buildings during the 1994 Northridge earthquake, and obtain consequence predictions via the FEMA P-58 methodology. The density of instrumentation examined ranges from the case in which all floors are instrumented to that in which no instrumentation is present and FEMA P-58 simplified procedures are used to predict response and corresponding consequences. We find that errors in consequences predictions decrease as the number of building instruments is increased and that the reduction in error is substantial as soon as more than a small number of floors are instrumented. This is valuable information for a building owner if they wish to use seismic instrumentation as a means of rapidly obtaining damage and loss information for post-earthquake decision-making.

Keywords: Seimic instrumentation, FEMA P-58 methodology, Seismic damage and loss predictions, Post-earthquake decision-making

1. Introduction

Recordings from instrumented structures have proven to be a valuable asset to the earthquake engineering community. They have contributed to the progression of design and analysis procedures, including code provisions [1]. Studies of instrumented buildings have enhanced understanding of the relationship between response and damage [e.g. 2, 3, 4, 5]. Instrumented responses can also facilitate decisions to retrofit the structural system [1, 6],

*Corresponding Author
URL: gcremen@stanford.edu (Gemma Cremen), bakerjw@stanford.edu (Jack W. Baker)
[1]Graduate Student, Department of Civil and Environmental Engineering, Stanford University
[2]Associate Professor, Department of Civil and Environmental Engineering, Stanford University

which can lead to reduced downtime following an earthquake [7]. Building instrumentation is considered so important that suggestions for its implementation have been made in building codes [e.g. 8].

In this study, we quantify the benefits of building instrumentation in a different context. We study the relationship between the level of seismic instrumentation present in a structure during a seismic event, and the accuracy of the resulting damage and loss consequence predictions according to the FEMA P-58 Seismic Performance Assessment procedure. It is important that these predictions are accurate as they can facilitate the post-earthquake decision-making and planning of building owners, such as rapidly evaluating whether a building can be re-occupied [9]. It is important to quantify the level of building instrumentation required for accurate consequence predictions, since one of the main limitations of building instrumentation is its large capital cost, making it largely uneconomical to install sensors on every level of a structure. Although attempts have been made to reduce these costs, for example by using wireless technologies [10, 11, 12, 13, 14, 15].

Few previous studies have explicitly related instrumentation to the Performance-based Earthquake Engineering (PBEE) framework, i.e. FEMA P-58, despite its potential for use in the required validation of PBEE technologies [16, 17]. Notable exceptions include [18, 19], who addressed how PBEE methods can be modified to incorporate accelerometer data from instrumented buildings to produce rapid estimates of repair cost, safety, and probable locations of physical damage. A key distinction between that work and our study is the manner in which the PBEE framework is modified to account for recorded responses; [18, 19] used Bayesian updating with observed sensor data to change the probability distribution of structural responses resulting from a nonlinear time-history analysis of a structural model, while we derive the structural responses directly from the sensor data. The work of [20, 21], in which a wavelet-based damage-sensitive feature is used with building geometric information to predict the building damage state at a given seismic intensity level, also demonstrated how instrumented buildings can facilitate rapid loss assessments. Another example of a study that combined sensor information with PBEE is [22], where recorded accelerations of a 24-story steel-frame building are used to compute story drift ratios that are then compared with the FEMA 273-style performance levels, i.e. 'Operational', 'Immediately Occupiable', 'Life Safety', and 'Collapse Prevention' [23]. Finally, [24] proposed a set of methodologies for automated post-earthquake damage assessment of instrumented buildings, using fragility functions to translate the recorded responses to damage levels that could be used to provide guidance on the threshold of motion that may necessitate inspection or evacuation of the building. However, these damage levels are consistent with the procedures of ATC-20 [25] rather than the performance levels associated with FEMA P-58.

1.1. PBEE Framework

The PBEE framework (FEMA P-58) combines ground motion hazard (IM - Intensity Measure), structural response (EDP - Engineering Demand Parameter), and prediction of component damage (DM - Damage Measure) to make a prediction of building loss (DV - Decision Variable) under earthquake loading. Note that IM, EDP, DM, and DV can be vectors. The methodology is probabilistic in nature, reflecting the uncertainty associated with seismic performance prediction. It is traditionally expressed in terms of the following

triple integral [26]:

$$\lambda(DV) = \iiint G(DV|DM)|dG(DM|EDP)|dG(EDP|IM)|\, d\lambda(IM)| \tag{1}$$

$G(DV|DM)$ is the complementary cumulative probability distribution function of DV conditioned on DM, i.e., $G(DV|DM) = p(DV \geq x_1|DM = x_2)$, while $|dG(DV|DM)| = f_{DV|DM}(x_1|x_2)dx_1$ is the conditional probability density function times dx_1. $G(DM|EDP)$ and $G(EDP|IM)$ are defined similarly. λ (.) is the mean annual rate of exceedance. Note that this is a time-based equation that considers all earthquakes and the frequencies of occurrence of resulting IMs within a 1-year period. We will focus on scenario-based and intensity-based assessments in this study, which deal with only one seismic event of interest. For these assessments, the framework may be more appropriately expressed as:

$$p(DV \geq x_1) = \iiint G(DV|DM)|dG(DM|EDP)|dG(EDP|IM)|f_{IM}(x_4)\, dx_4 \tag{2}$$

and the exceedance probability for damage can be expressed as:

$$p(DM \geq x_2) = \iint G(DM|EDP)|dG(EDP|IM)|f_{IM}(x_4)\, dx_4 \tag{3}$$

1.2. Seismic Instrumentation and PBEE

Let N be the number of floors (including the roof) in a structure and n the number of floors with seismic instrumentation. Possible seismic instrumentation density in the structure can be divided into 3 categories: $n = 0$ (no instrumentation), $0 < n < N$ (partial instrumentation), and $n = N$ (full instrumentation).

When $n = 0$, neither the IMs nor the EDPs are measured for the structure in a seismic event. Thus, there is uncertainty in all four variables of the PBEE framework. Exceedance probabilities for damage and loss can be calculated from equations 2-3.

When $0 < n < N$, there is at least ground floor instrumentation present in the structure, which we assume eliminates uncertainty in the IMs. (Note that this could be a simplifying assumption if there is considerable soil-structure interaction). There is still uncertainty in the EDPs, which depends on the number of floors instrumented. Damage and loss predictions are thus dependent on the ground motion measured ($n = 1$ only) and the level of instrumentation present in the structure. Damage and loss exceedance probabilities can be expressed as follows:

$$p(DM \geq x_2) = \int G(DM|EDP)f_{EDP}(x_3)\, dx_3 \tag{4}$$

and

$$p(DV \geq x_1) = \iint G(DV|DM)|dG(DM|EDP)|f_{EDP}(x_3)\, dx_3 \tag{5}$$

When $n = N$, both the IMs and all EDPs are measured during a seismic event, eliminating their uncertainty (note that this is an idealized assumption for drift-related EDPs, since there will be error due to double integration). Damage and loss exceedance probabilities can be expressed as follows:

$$p(DM \geq x_2) = G(DM|EDP) \tag{6}$$

and

$$p(DV \geq x_1) = \int G(DV|DM)|dG(DM|EDP)| \tag{7}$$

By reducing or eliminating uncertainty in some of the random variables in equations 2-3, seismic instrumentation in a building should reduce the uncertainty and increase the accuracy of consequence predictions calculated according to the FEMA P-58 methodology for a building in a given seismic event.

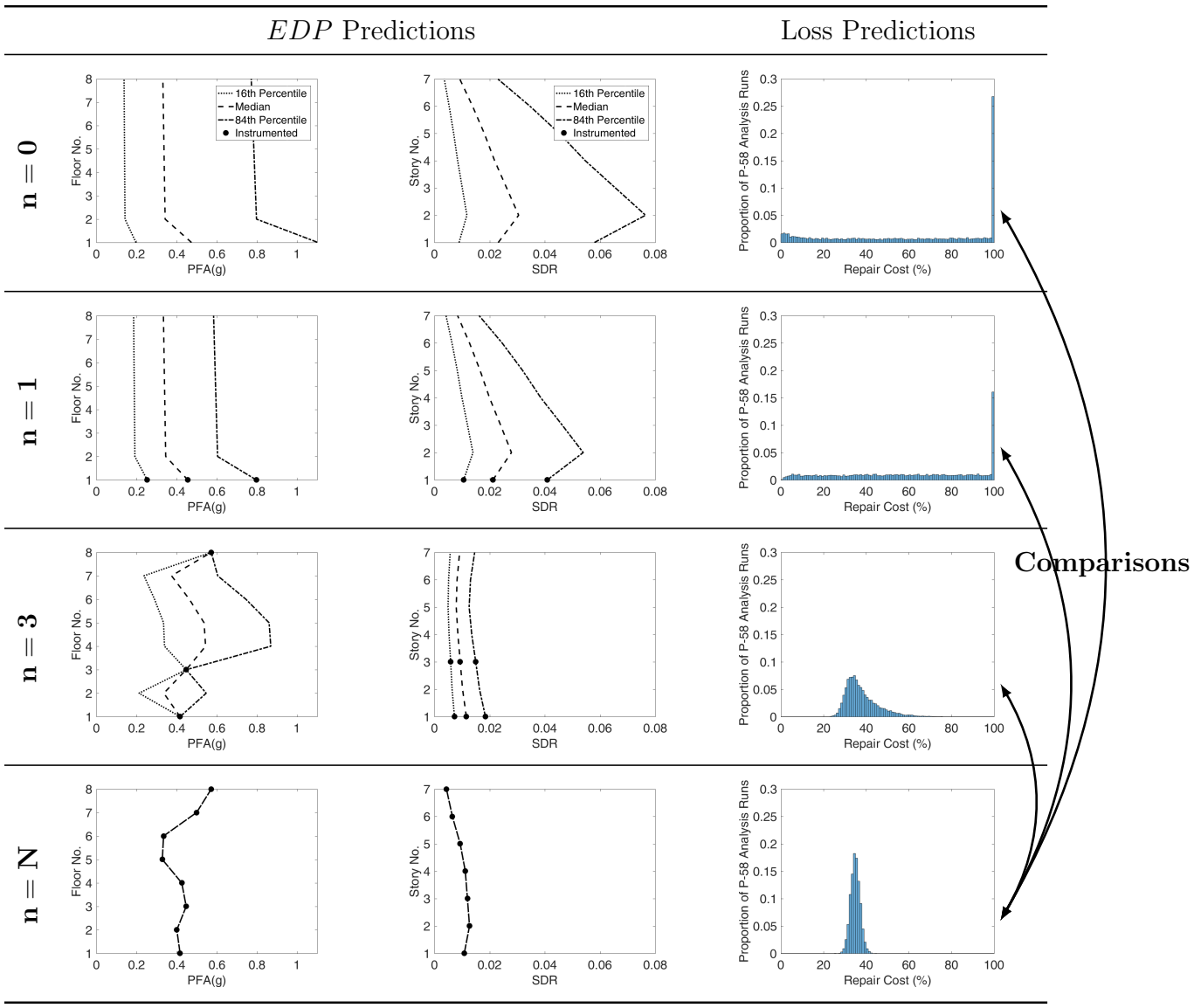

Figure 1: Graphical summary of the benchmarking procedure.

2. Methodology

We examine a building of interest subjected to a given seismic event. The building has N floors (including the roof), n of which have seismic instrumentation. We vary the level of instrumentation present in the building and investigate the effect on uncertainty in the building's damage and loss predictions for the considered seismic event from the FEMA P-58 methodology, by benchmarking the predictions against those of the fully instrumented case ($n = N$). We use the SP3 software tool [27] to run the FEMA P-58 analyses.

We assume the ground floor is always instrumented for $n > 0$, and the roof is always instrumented for $n > 1$. We examine all possible locations of other instruments for each level of instrumentation in this study. The optimal layouts of instrumentation suggested by previous studies [e.g. 28, 29, 30, 31, 32, 33, 34] have not been optimized specifically for accuracy in FEMA P-58 damage and loss predictions, so no guidance exists yet for the given situation. Figure 1 provides a graphical summary of the benchmarking procedure. It involves the following steps:

1. Define the IM and EDP inputs:
   - I. Determine the IMs (if $n \leq 1$).
   - II. Determine the EDPs.
   - III. Determine uncertainty in the EDPs.
   - IV. Determine correlation between the EDPs.
2. Run the P-58 analysis using the IM and EDP inputs.
3. Benchmark the damage and loss predictions of interest.

These steps are described in greater detail in the following subsections.

2.1. Determine the IMs

IMs are explicitly considered for $n \leq 1$, where they are used as inputs to the FEMA P-58 simplified analysis method. For all other values of n, IMs are only implicitly accounted for in the EDPs at the ground floor. IMs of interest for $n \leq 1$ are the peak ground acceleration (PGA) and the 5% damped spectral acceleration at the building's fundamental period, $Sa(T)$.

When $n = 0$, IM values are the median values obtained from a ground motion prediction equation. The fundamental period is assumed to be the average of the periods in the two orthogonal directions. Uncertainty in the values is included as an uncertainty in the EDPs (β_{gm} in Section 2.3). The selection of an appropriate ground motion prediction equation may be site or region specific and is therefore left to each individual user of the methodology.

When $n = 1$, the IMs are assumed to be captured by the instruments on the ground floor. PGA is taken to be the largest absolute value of acceleration recorded at the ground floor in either orthogonal direction. The value of $Sa(T)$ is the value recorded on the same instrument as the PGA, at the fundamental period of the building in the direction of the instrument. No uncertainty is applied to the values, since they are directly measured.

2.2. Determine the EDPs

The EDPs considered are story drift ratio (SDR) and peak floor acceleration (PFA). PFA at floor i in a given orthogonal direction is defined as the maximum absolute acceleration in the time series for that floor, i.e.

$$PFA_i = max|a_i(t)| \tag{8}$$

where $a_i(t)$ is the acceleration at floor i for time t. SDR at story i in a given orthogonal direction is obtained from the displacement time series for that floor and the adjacent floor, according to the following equation:

$$SDR_i = \frac{max|d_i(t) - d_{i+1}(t)|}{hs_i} \tag{9}$$

where $d_i(t)$ is the displacement at floor i for time t and hs_i is the height of story i. When $n = N$ (the benchmark case), PFA and SDR are obtained from the instrumented values of $a_i(t)$ and $d_i(t)$ at each floor. If the building does not contain instruments in each orthogonal direction on all floors, we assume the true values of $a_i(t)$ and $d_i(t)$ at non-instrumented floors are those obtained using cubic spline interpolation of the data time series at instrumented floors. Note that this may be a simplifying assumption, but the technique has been used in previous studies to recover structural demands at non-instrumented floors [29, 35]. A cubic spline is a third-order polynomial of the form:

$$f(h_i) = ah_i^3 + bh_i^2 + ch_i + d \tag{10}$$

where h_i is the height of floor i relative to the ground, $f(h_i)$ is $a_i(t)$ or $d_i(t)$, and a,b,c are coefficients obtained by forcing the $f(h_i)$ values and their derivatives to be equal at each floor when calculated from adjacent stories. We implement the simple and popular "not-a-knot" version of spline interpolation, which requires the third derivative of the spline to be continuous at both the second lowest and second highest instrumented floors [36].

When $n \leq 1$, median EDPs are predicted from the IMs, using the FEMA P-58 simplified analysis method [9]. Note that this method has a number of simplifying assumptions and may not be reliable in certain cases (see Appendix C for additional details). When $n > 1$, EDPs fully constrained by instrumented data time series are equivalent to the corresponding EDPs of the benchmark case. When $1 < n < 4$, we obtain $a_i(t)$ and $d_i(t)$ at non-instrumented floors using not-a-knot cubic spline interpolation of the data time series at instrumented floors. Relevant EDPs are then derived from these values. When $n \geq 4$, we have a sufficient number of instruments available to use the jackknife re-sampling technique [37] to recover median EDP predictions not fully constrained by instrumented data. This technique has been used extensively in previous studies to quantify errors and uncertainties in interpolated data [38, 39, 40, 41, 42]. For these cases, the median EDP prediction of interest ($\widetilde{r}$) is obtained as follows:

1. Generate n-2 jackknife samples. Each jackknife sample contains the relevant data time series from n-1 of the available instruments, with a different set of non-boundary instrumented data being omitted from each sample. Data from the boundary instruments are included in each sample to facilitate the cubic spline interpolation carried out in the next step.

2. For each jackknife sample, estimate $a_i(t)$ and $d_i(t)$ at non-instrumented floors using not-a-knot cubic spline interpolation of the available instrumented data time series. Use these estimates to compute the EDP parameter of interest (r_i).

3. Compute the logarithmic mean of all n-2 samples of r_i, $\bar{x}_{\ln r}$.

4. Compute $\widetilde{r}$: $\widetilde{r} = e^{\bar{x}_{\ln r}}$.

2.3. Determine Uncertainty in the EDPs

When $n = N$, there is no uncertainty in the EDPs, since they are directly measured. When $n < N$, we apply three different types of uncertainty to median EDPs: record-to-record variability (β_a), epistemic uncertainty (β_u), and ground motion uncertainty (β_{g_m}). Note that these are all log standard deviations. The uncertainties are applied to EDPs at all floors when $n \leq 1$, in line with the P-58 simplified analysis method, and EDPs not fully constrained by instrumented data when $n > 1$.

When $n \leq 1$, β_a is equivalent to the values of record-to-record variability included in a FEMA P-58 simplified analysis method for the building. β_a may differ between PFA and SDR, and in both orthogonal directions of the building. Values are applied directly in line with the P-58 simplified analysis method when $n \leq 1$. When $1 < n < 4$, we do not have a method of quantifying this uncertainty as we only have one set of interpolated EDP values, so it is estimated as the average of all β_a values for $n \leq 1$. When $n \geq 4$, this uncertainty measure is a quantification of uncertainty in the interpolation used in the jackknife re-sampling process. It is calculated as follows:

$$\beta_a = \sqrt{\frac{\sum_{i=1}^{n-2}(\ln(r_i) - \bar{x}_{\ln r})^2}{n-3}} \tag{11}$$

where r_i is the estimate of the EDP parameter of interest for the ith jackknife sample and $\bar{x}_{\ln r}$ is the logarithmic mean of the n-2 jackknife samples of r_i.

β_u is equivalent to the P-58 simplified analysis method modeling uncertainty when $n \leq 1$. When $n > 1$, we include a number of different values for this measure in our analyses ranging from 0.1 to the value applied when $n \leq 1$, and leave the final selection to the user's judgment. Note that β_u could also be applied to EDPs fully constrained by instrumented data for cases where instruments are not believed to provide perfect measurements of EDPs, however we do not consider such cases in this study.

β_{g_m} is only non-zero when $n = 0$. It is equivalent to the uncertainty in $S_a(T)$ computed from the ground motion prediction equation used to obtain the median IM values.

Note that the total log standard deviation of EDP input to the P-58 analysis is an aggregation of the different types of EDP uncertainties computed, using the sum of the squares rule because the various contributions to uncertainty are independent:

$$\beta = \sqrt{\beta_a^2 + \beta_u^2 + \beta_{gm}^2} \tag{12}$$

2.4. Determine Correlation between the EDPs

When $n = N$, the correlation matrix is irrelevant since there are no EDP uncertainties. Perfect correlation is assumed between EDPs when $n \leq 1$, in line with the P-58 simplified analysis method. When $n > 1$, the correlation matrix is estimated using the logarithm of all N-2 sets of median EDPs for $n = 3$ (note that this correlation matrix cannot be computed for $N = 3$; in this case when $n = 2$, a reasonable correlation matrix should be estimated from a reliable source, e.g. an analysis of the building under multiple ground motions).

2.5. Run the P-58 Analysis using the IM and EDP inputs

The EDP inputs are used as parameters in a multivariate normal distribution of $lnEDP$. The mean vector (μ) and covariance matrix (Σ) of the $lnEDP$ distribution can be expressed as follows:

$$\mu = \ln(\widetilde{R}) \tag{13}$$

and

$$\Sigma = \beta \times \rho \times \beta \tag{14}$$

where $\widetilde{R}$ is the set of all median EDPs, β is the diagonal matrix of log standard deviations of EDPs, and ρ is the correlation matrix of the $lnEDP$s. Simulated $lnEDP$s are sampled from the multivariate normal distribution with parameters given by equations 13-14 for each run of the P-58 Analysis.

All components in the building should be specified, as they are needed to predict damage. DMs are calculated in a probabilistic manner for the given set of simulated EDPs, using fragility functions for each component. (Note that we assume the building has not collapsed and does not experience residual drift). Each function represents the probability of occurrence of a particular damage state of a component, conditioned on the magnitude of the associated EDP. Possible components of interest are those that could cause the building to be assigned an unsafe placard, since an error in their damage prediction could give a false initial indication of the building's level of safety. Each fragility function is associated with a statistical distribution of repair costs, repair time, and casualties, which are equivalent to DVs.

2.6. Benchmark the Damage and Loss Predictions of Interest

The sets of damage and loss predictions of interest are then benchmarked against the corresponding sets of predictions calculated for $n = N$. An error metric that can be used to benchmark predictions is:

$$\text{Error} = \sqrt{\frac{\sum_{i=1}^{n_s}(\bar{L} - \hat{L}_i)^2}{n_s}} \tag{15}$$

where $\hat{L}_i$ is the predictions of interest for the ith P-58 Monte Carlo sample, $\bar{L}$ is the mean of all $\hat{L}_i$ when $n = N$, and n_s is the number of Monte Carlo samples. Note that this metric results in a non-zero error for the $n = N$ case, as the EDPs are assumed known but not the resulting loss.

3. Application

To illustrate the methodology outlined in the previous section, we consider a specific building and seismic event. The building of interest is the Van Nuys hotel building in its condition prior to the 1994 Northridge earthquake, which has been extensively studied in previous work [e.g. 43, 5, 44]. We study the instrumented response of the building to the 1994 Northridge earthquake (M_w 6.7) and examine two P-58 consequence predictions. The building is a 7-story reinforced concrete structure (Figure 2). Further details on its construction can be found in Table A.2. The replacement value is the default set by the SP3 program based on the building's occupancy type, and we assume a total loss threshold of 100%. It is seismically instrumented at floors 1, 2, 3 and 6, as well as at the roof. We only use one set of instruments (listed in Table A.2) in each orthogonal direction in the building to capture the response (i.e. we ignore torsional effects). We hypothetically add and remove instruments from the building, examining all levels of instrumentation from $n = 0$ to $n = N$. To "add" instruments to the building, we interpolate the data time series at instrumented floors and treat the interpolated results as true (as discussed in Section 2.2).

3.1. IM and EDP Inputs

IM and EDP inputs are obtained according to the methodology in the previous section, using data from [45]. When $n \leq 1$, the parameter values used in the FEMA P-58 simplified analysis method are the default values for the building calculated by the SP3 program (see Table C.4). When $n = 0$, the [46] ground motion prediction equation is used to compute the IM predictions. Values used for the parameters of the equation are found in Table B.3. Earthquake parameter values are obtained directly from the NGA-West2 database [47]. Distance parameter values used are those of the nearest recording station in the NGA-West2 database (located 3.2 km from the site). The V_{S30} value for the site is obtained from a previous study of the building [48]. Average uncertainties in the median EDPs for each level of instrumentation are summarized in Table 1.

Table 1: Average EDP uncertainties for different levels of instrumentation.

Level of Instrumentation	$\boldsymbol{\beta}_a$	$\boldsymbol{\beta}_u$	$\boldsymbol{\beta}_{g_m}$
$n = 0$	0.36	0.5	0.65
$n = 1$	0.36	0.5	0
$n = 2$	0.36	0.1-0.5	0
$n = 3$	0.36	0.1-0.5	0
$n = 4$	0.16	0.1-0.5	0
$n = 5$	0.07	0.1-0.5	0
$n = 6$	0.02	0.1-0.5	0
$n = 7$	0.01	0.1-0.5	0
$n = N$	0	0	0

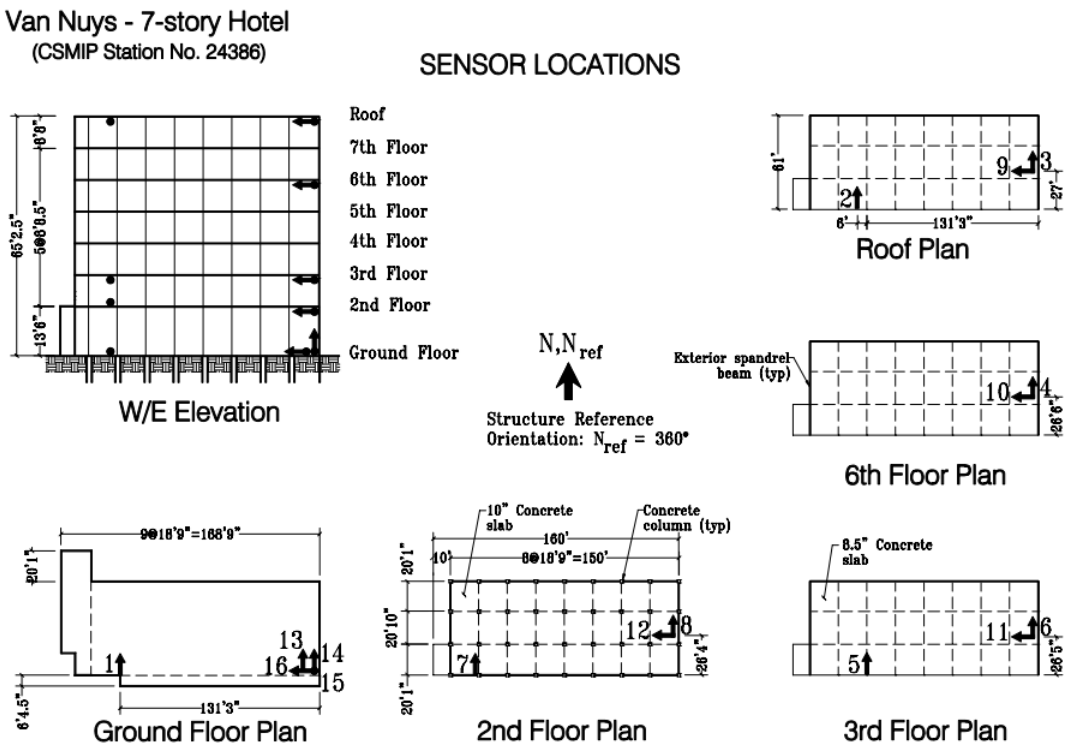

Figure 2: Details of the Van Nuys hotel building [45].

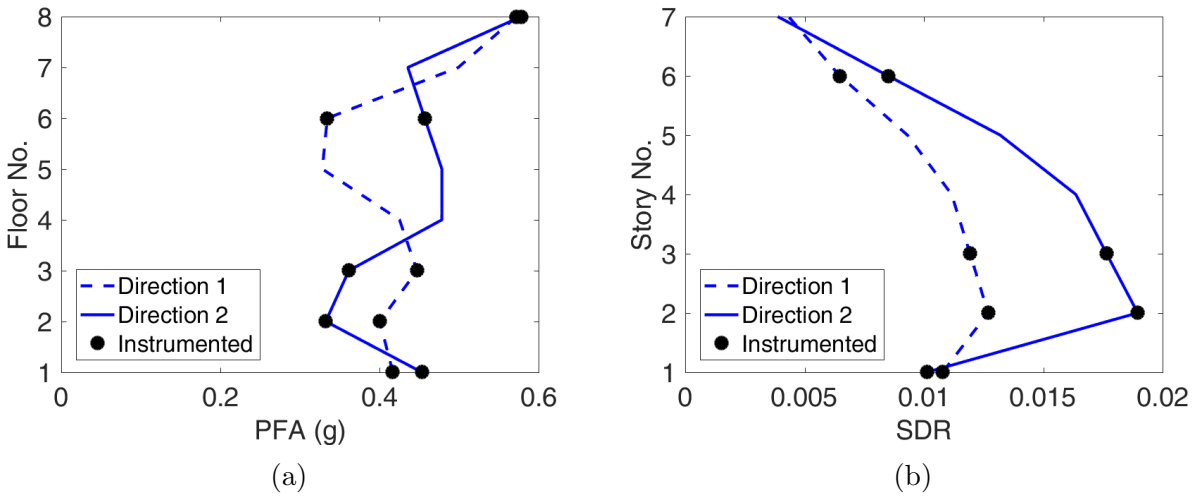

Figure 3: (a) Peak floor acceleration and (b) story drift ratio of the Van Nuys Hotel building when $n = N$.

3.2. P-58 Analysis

10000 Monte Carlo samples are used in each P-58 analysis. The damage prediction of interest is the mean damage state of curtain walls per story in a given orthogonal direction:

$$\bar{ds}_{f,a} = \frac{\sum_{i=0}^{2} DS_i \times c_{f,a,i}}{m_{f,a}} \tag{16}$$

where $\bar{ds}_{f,a}$ is the mean damage state of curtain walls in story f in the orthogonal direction a, DS_i is the number of damage state i, $c_{f,a,i}$ is the number of units of the curtain wall component in story f in the direction a in DS_i, and $m_{f,a}$ is the total number of units of the curtain wall component in story f in the direction a. The curtain wall component in the building model has Fragility ID 'B2022.002' under the P-58 methodology. This type of curtain wall has two damage states, in addition to the occurrence of no damage. The first damage state involves the cracking of glass and the second damage state involves the falling of glass from its frame. This component is of interest because the second damage state has the potential to cause an unsafe placard to be assigned to the building. The loss prediction of interest is the building repair cost:

$$\text{Building Repair Cost (\%)} = \frac{\sum_{i=1}^{k} RC_i}{\text{Building Replacement Cost}} \times 100 \tag{17}$$

where RC_i is the repair cost associated with the ith component and k is the total number of components within the building.

3.3. Benchmarking Damage and Loss Predictions

3.3.1. Mean Damage State of Curtain Walls

We use equation 15 to benchmark predictions, with $\hat{L}_i$ representing the P-58 curtain wall mean damage state prediction for a given story in a given orthogonal direction for the ith Monte Carlo sample. Figure 4 shows the range of error in the prediction of the mean damage state of curtain walls in the longer direction of the building across the seven stories of the building for different values of n, when $\beta_u = 0.5$. The error values plotted for a given story and a given value of n are the minimum and the mean across all combinations of instrumentation for that value of n.

Errors in the prediction of the mean damage state of curtain walls per story in the longer direction of the building are significant for $n \leq 1$, but the minimum errors become negligible for $n > 3$. Note the small range of errors obtained when $n = 2$. This is because the variance dominates the error for this value of n, and values of the variance are very similar for all stories since the median SDR and its uncertainty are identical at all stories for this value of n. Similar results are observed for different values of β_u.

Figure 5 shows the range of error in the prediction of the mean damage state of curtain walls in the longer direction on the 5th story for different values of n, when $\beta_u = 0.5$. Errors for combinations of instrumentation that involve instrumenting both the 5th and 6th floor are negligible compared to errors for combinations of instrumentation in which instruments are omitted from either the 5th or 6th floor, independent of the value of n. This makes intuitive sense, since the median EDP predictions on the 5th story are only influenced by

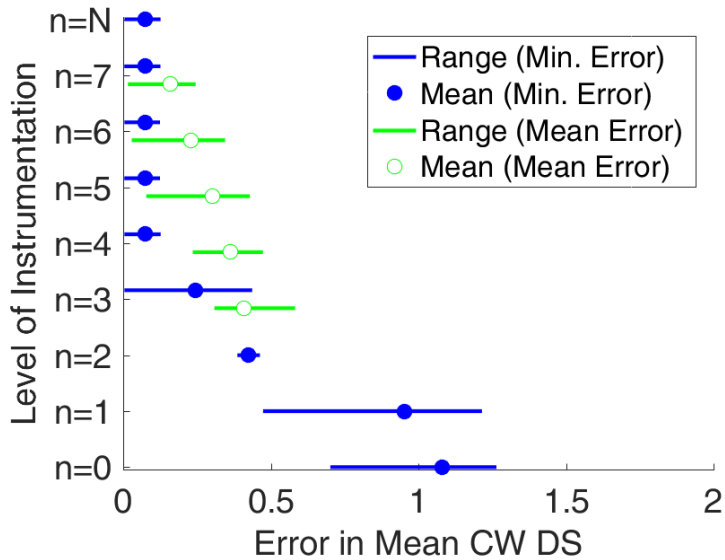

Figure 4: Ranges of error in the mean damage state of curtain walls per story in the longer direction, when $\beta_u = 0.5$.

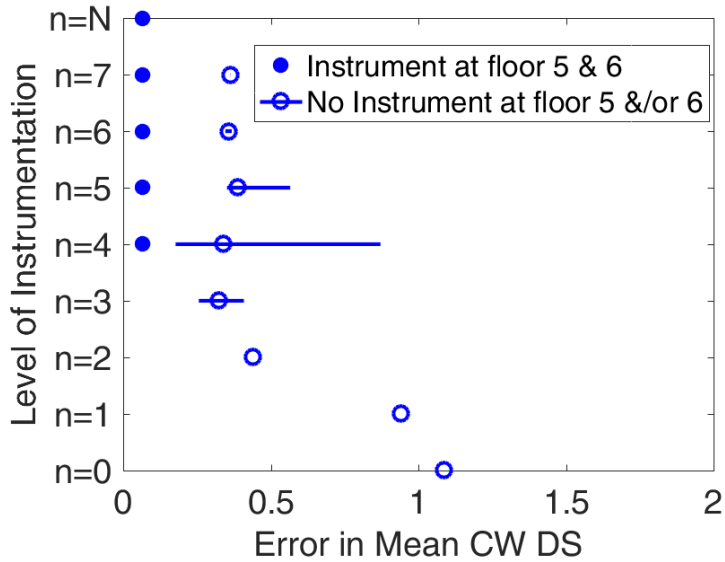

Figure 5: Ranges of error in the mean damage state of curtain walls on the 5th story in the longer direction, when $\beta_u = 0.5$. Note that there cannot be instruments at both the 5th and 6th floors when $n = 3$, since the ground floor and the roof are always instrumented.

the presence of instrumentation on the 5th floor and the 6th floor. In addition, the size of the error ranges for combinations of instrumentation in which instruments are omitted from either the 5th or 6th floor vary significantly for different values of n. We can conclude that adding instrumentation does not always result in a lower error in the prediction of the mean damage state of curtain walls on a given story, and the sensitivity of the prediction error to different instrumentation layouts differs between different values of n. Similar results are observed for other values of β_u.

3.3.2. Building Repair Cost

We use equation 15 to benchmark predictions, with $\hat{L}_i$ denoting the P-58 building repair cost prediction for a given arrangement of instrumentation at a given value of n for the ith Monte Carlo sample. Figure 6 provides histograms of $\hat{L}_i$ for a given arrangement of instrumentation at each value of n, when $\beta_u = 0.5$. Figure 6 indicates that there is an

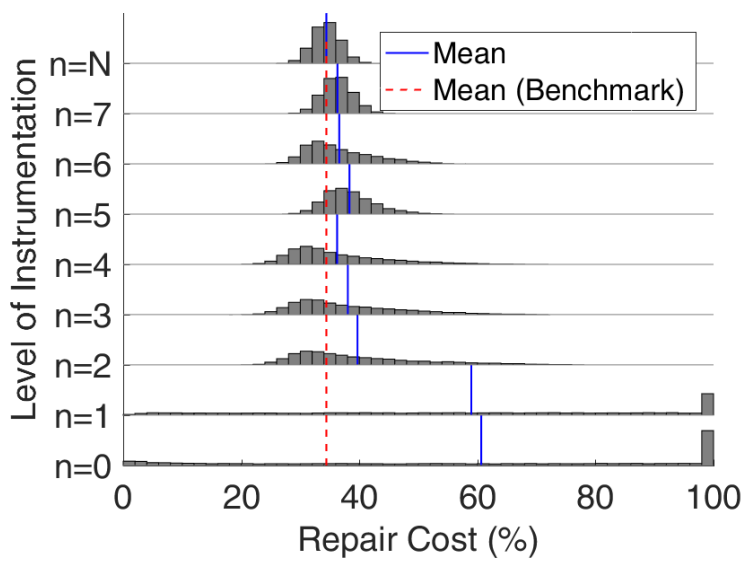

Figure 6: Histograms of building repair cost predictions, when $\beta_u = 0.5$.

overall decrease in building repair cost prediction error as the number of instruments in the building is increased. The prediction error is significantly larger for $n \leq 1$ than for all other values of n. A summary of the error in building repair cost prediction across the total range of n is found in Figure 7 for various values of β_u. Both the minimum and the mean error values across all combinations of instrumentation are plotted for a given value of n. The error in building repair cost generally decreases as n increases and the errors associated with $n \leq 1$ are notably larger than the errors associated with any other value of n, across all values of β_u examined.

Figure 8 shows the range of error in building repair cost predictions across all combinations of instrumentation for different values of n, when $\beta_u = 0.5$. Values of $n < 3$ are not included, since each value of n in this case is associated with only one combination of instrumentation and the error can be obtained from Figure 7. It can be seen that the size of the error ranges vary across the different values of n. For example, the difference between

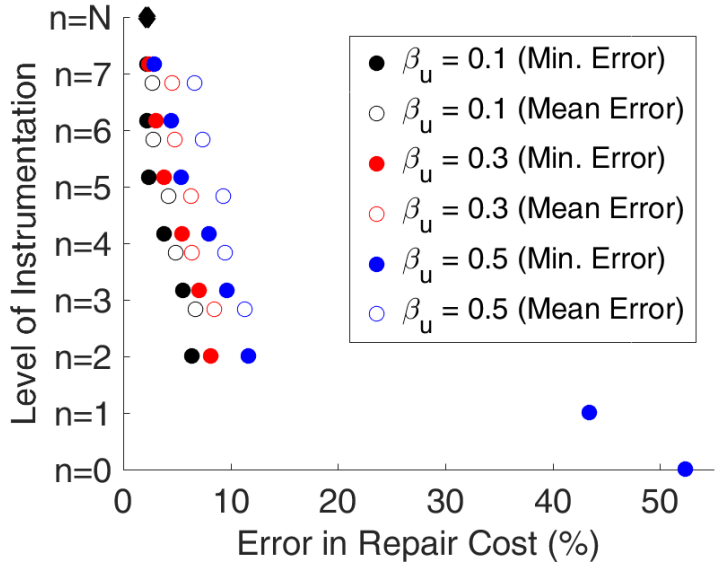

Figure 7: Summary of building repair cost prediction error.

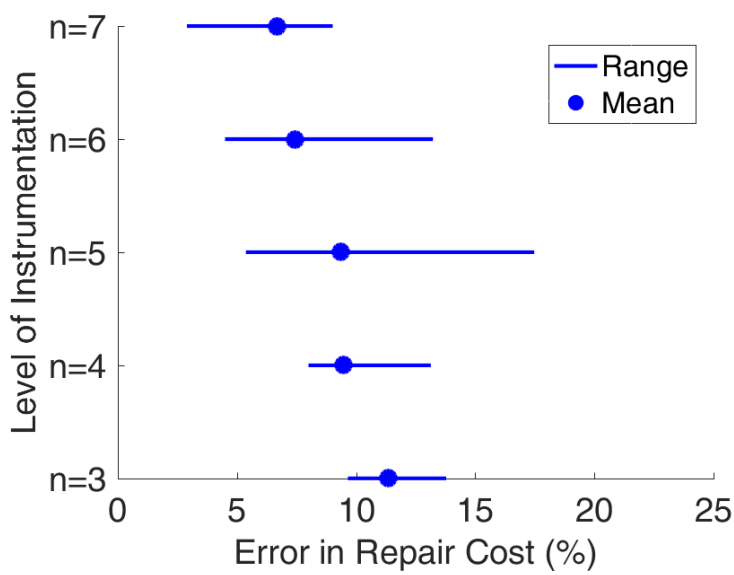

Figure 8: Ranges of building repair cost prediction error, when $\beta_u = 0.5$.

the maximum and minimum error is approximately 4.1% when $n = 3$, whereas it is approximately 12.1% when $n = 5$. The sensitivity of the error in building repair cost predictions to different instrumentation layouts for a given n is therefore dependent on the value of n. It is interesting to note that the maximum error associated with $n = 5$ is larger than errors for both $n = 4$ and $n = 3$. This is because the cubic spline interpolation method fortuitously leads to more accurate EDP predictions when $n = 4$ and $n = 3$, than for certain cases when $n = 5$. Thus, adding instrumentation does not always guarantee a lower error in the building repair cost prediction, according to our methodology. Similar results are observed for different values of β_u.

3.4. Sensitivity to EDP Inputs

To determine whether the above damage and loss predictions are consistent across other events, we double EDPs and examine the effect this has on the errors of the consequence predictions associated with different values of n, keeping everything else about the analyses constant. (Note that this is only an idealized approximation of the building response to a higher seismic intensity level, as we do not have building response data for any other event).

For $n \leq 1$, we multiply the IM inputs by two and use these updated values to compute new median EDP predictions according to the P-58 simplified analysis method. For $n > 1$, we modify the EDPs by simply doubling the median EDP predictions input to the P-58 analysis. Values of β_u and β_{g_m} are unchanged. The average value of β_a is 0.35 for $n < 4$, in line with the P-58 simplified analysis method for the updated strength ratio of the structure. Values of β_a are unchanged for $n \geq 4$.

Figure 9(a) compares the errors in the prediction of the mean damage state of curtain walls in the longer direction of the building on the 5th story of the building, for all values of n and β_u =0.5. There are non-negligible differences in mean damage state prediction errors for most values of n. We can conclude that the magnitude of the error is sensitive to the response of the building for certain values of n. However, the general pattern of error across the different values of n is similar for both sets of EDPs.

Figure 9(b) compares the errors in building repair cost predictions for both sets of building EDPs across all values of n, when $\beta_u = 0.5$. It can be seen that differences in building repair cost prediction error are negligible for $n \geq 2$, but there is a difference of approximately 15% for $n \leq 1$. However for both sets of EDPs, the error is generally decreasing as n increases and is significantly larger for $n \leq 1$ than any other value of n.

4. Additional Application

To further exercise our methodology, we apply it to a significantly different second building for the same event and examine if similar trends in repair cost prediction error are observed. The building of interest is a 17-story residential reinforced concrete structure (Figure 10) located in Los Angeles, that was also shaken in the Northridge earthquake. Further details on its construction can be found in Table A.2. The replacement value is the default set by the SP3 program based on the building's occupancy type, and we assume a total loss threshold of 100%. The building is seismically instrumented at floors 1,7, and 13, as well as at the roof. We only use one set of instruments (listed in Table A.2) in each orthogonal direction in the building to capture the response (i.e. we ignore torsional effects).

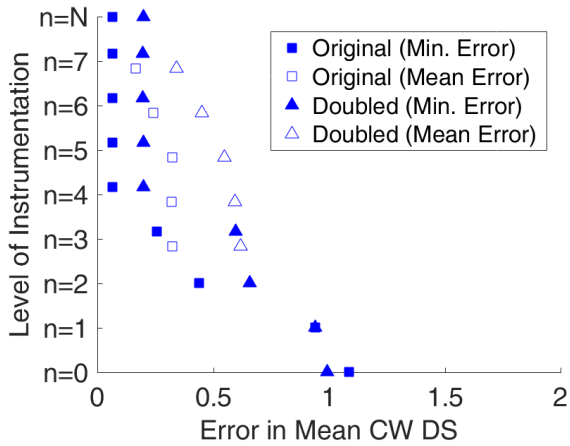

(a)

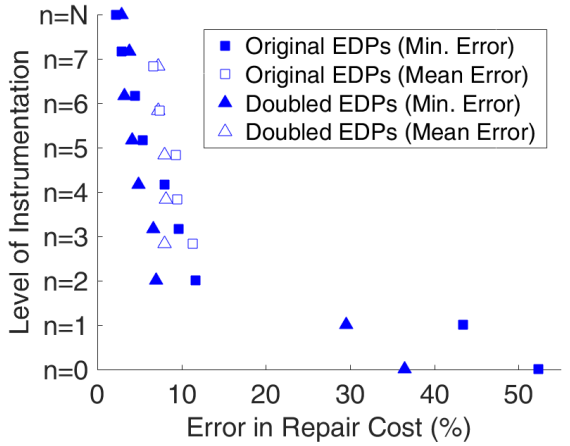

(b)

Figure 9: Errors in predictions of (a) damage state of curtain walls on the 5th story in the longer direction and (b) building repair cost, for both sets of EDPs when $\beta_u = 0.5$.

We hypothetically add and remove instruments from the building, investigating five levels of instrumentation ($n = 0$ to $n = 3$, and $n = N$).

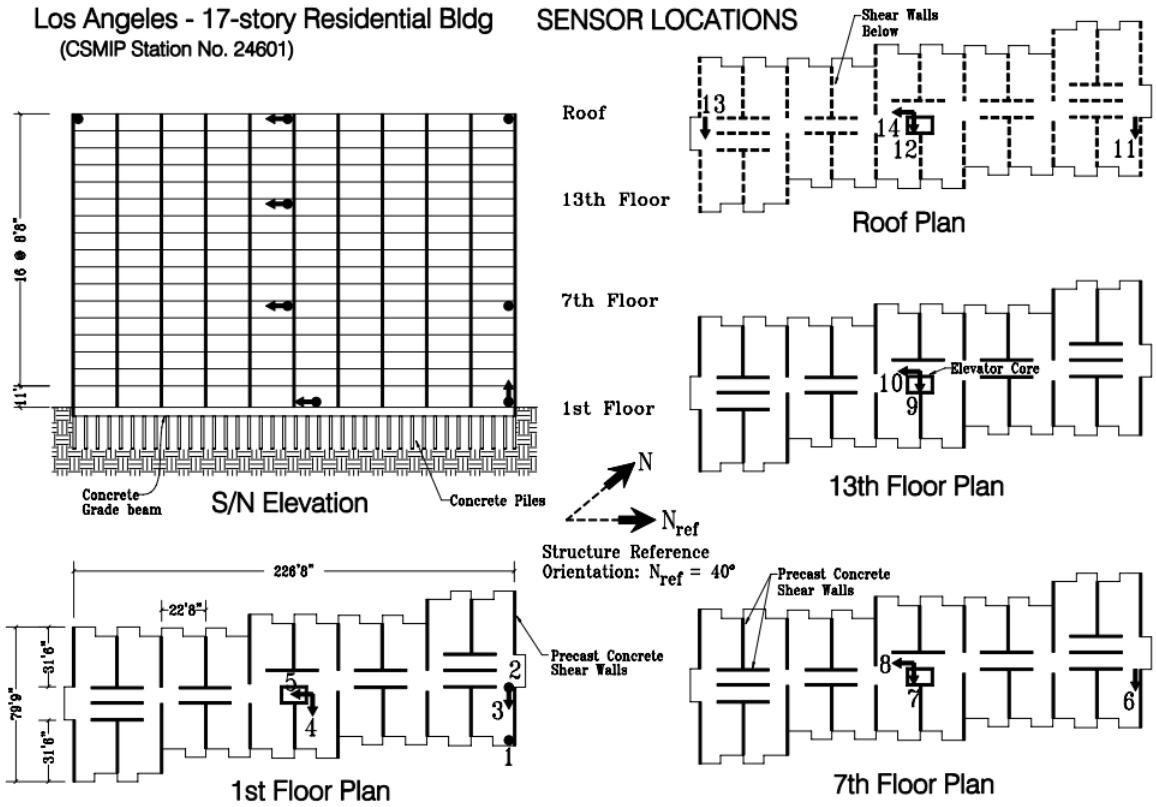

Figure 10: Details of the residential building [45].

4.1. IM and EDP Inputs

IM and *EDP* inputs are obtained according to the methodology, using data from [45]. When $n \leq 1$, the parameter values used in the FEMA P-58 simplified analysis method are the default values for the building calculated by the SP3 program (see Table C.4). Note that the number of stories in the building exceeds the upper limit for which the P-58 simplified analysis method was calibrated, however the median *EDP*s predicted for the building were judged to be reasonable. When $n = 0$, we used the [46] ground motion prediction equation to compute the *IM* predictions. Values used for the parameters of the equation are found in Table B.3. Earthquake parameter values are identical to those used for the Van Nuys hotel building. Distance parameter values and the V_{S30} value used are those of the nearest recording station in the NGA-West2 database (located 692 m from the site). The equation yields a value of 0.68 for β_{gm}. The average value of β_a used is 0.21 when $n = 0$, 0.31 when $n = 1$, and 0.26 when $1 < n < 4$, and the value of β_u is 0.25 when $n \leq 1$, all in accordance with the P-58 simplified analysis method. Note that these uncertainties are smaller than those calculated according to the P-58 simplified analysis method for the Van Nuys building, since there is less non-linearity of the strength ratio in this case. We investigate values for β_u of 0.1 and 0.25 at other values of n.

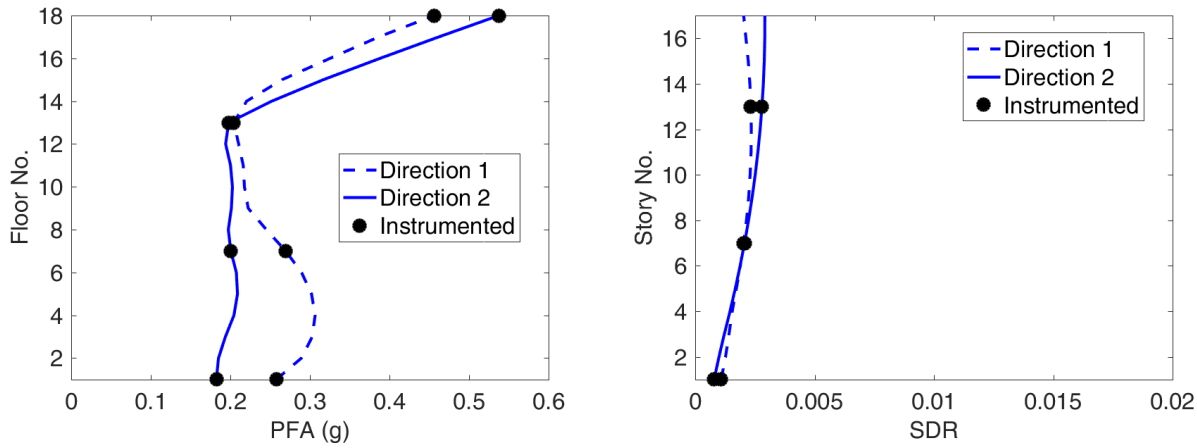

(a) (b)

Figure 11: (a) Peak floor acceleration and (b) story drift ratio of the residential building for $n = N$.

4.2. P-58 Analysis

10000 Monte Carlo samples are used in each P-58 analysis. We examine the set of building repair cost predictions for this building.

4.3. Benchmarking Loss Predictions

We use the same error metric to benchmark the repair cost predictions (Equation 15). Figure 12(a) provides histograms of $\hat{L}_i$ for a given arrangement of instrumentation at each value of n examined, when $\beta_u = 0.25$. The figure indicates that there is generally a decrease in building repair cost prediction error as the number of instruments in the building is increased, similar to the Van Nuys hotel building. Figure 12(b) summarizes the error in building repair cost prediction across each value of n examined, for the two values of β_u. Both the minimum and the mean error values across all combinations of instrumentation are plotted for a given value of n. The error in building repair cost prediction tends to decrease as n increases and the errors associated with $n \leq 1$ are larger than the errors associated with any other value of n, across both values of β_u examined. The trend in error is very similar to that observed for the Van Nuys hotel building.

5. Conclusions

This study provides a method for quantifying the benefits of building instrumentation, by measuring errors in damage and loss consequence predictions calculated from the FEMA P-58 Seismic Performance Assessment procedure, when different numbers of building instruments are used to capture the response of the structure in a given event. The accuracy of these predictions is important to quantify, as they can be used to facilitate the post-earthquake decision-making and planning of building owners. The density of instrumentation examined ranges from the case in which all floors are instrumented to that in which no instrumentation is present and FEMA P-58 simplified procedures are used to predict response and corresponding consequences.

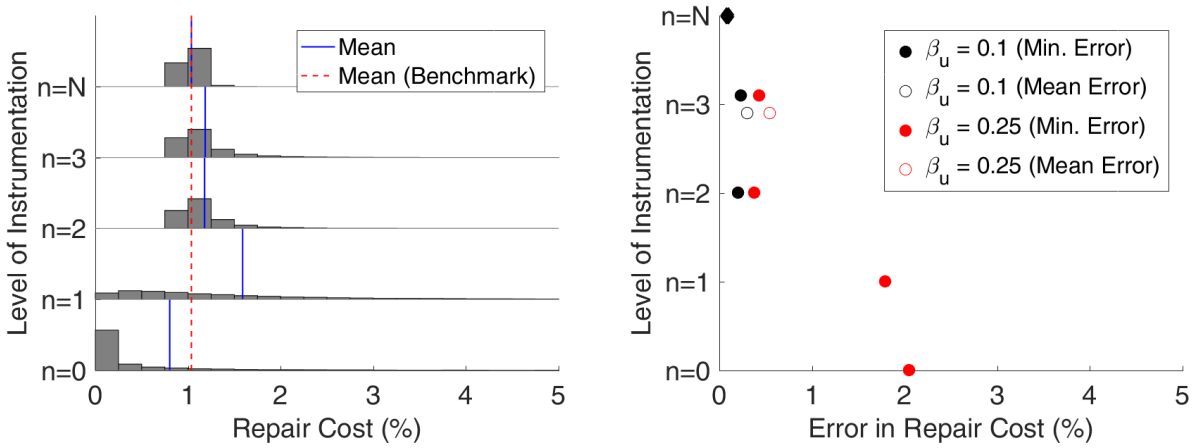

Figure 12: (a) Histograms of building repair cost predictions, when β_u =0.25. (b) Summary of building repair cost prediction error.

We have demonstrated the methodology by applying it to a 7-story structure for two different sets of seismic responses. We used the methodology to measure the error in predictions of the mean damage state of curtain walls per story in a given orthogonal direction and building repair cost, when different numbers of building instruments are used to record responses. To further exercise the methodology, we have also applied it to a building with significantly different properties. We quantified the errors in the same loss prediction for varying levels of instrumentation and observed similar trends in these errors to those of the other structure.

The errors in consequence predictions tend to decrease as the number of building instruments is increased, and the reduction in error is substantial as soon as more than a small number of floors are instrumented. This conclusion may only hold for certain arrangements of instruments at the different levels of instrumentation, however. It is therefore not crucial to have a very high density of instrumentation to obtain reasonable accuracy in FEMA P-58 consequence predictions for a building, but the accuracy achieved for the chosen level of instrumentation may be highly dependent on the arrangement of instruments within the building. The optimum arrangement of instruments for a given level of instrumentation depends on the consequence prediction of interest. For example, if the consequence is only dependent on the drift of the 5th story, instrumentation arrangements that include instrumenting the 5th and 6th floors will yield lower consequence prediction errors than instrumentation arrangements that do not include instrumenting these stories.

The above findings provide actionable information for a building owner if they wish to use seismic instrumentation as a means of rapidly obtaining damage and loss information for post-earthquake decision-making.

6. Acknowledgements

We thank three anonymous reviewers for helpful feedback that improved the quality of this manuscript. We thank Dr. Farzad Naeim for providing a copy of the SMIP Information

System. An academic license of the SP3 software (*www.hbrisk.com*) was used to perform P-58 analyses, and we are very grateful to Kate Fizgerald Wade at HB-Risk for all her assistance with this software.

7. Bibliography

[1] M. Çelebi, Seismic instrumentation of buildings, US Department of the Interior, US Geological Survey, 2000.

[2] F. Naeim, R. Lobo, Performance of non-structural components during the January 17, 1994 Northridge earthquake–case studies of six instrumented multistory buildings, in: Proceedings of the Seminar on Seismic Design, Retrofit, and Performance of Nonstructural Components, ATC-29-1, San Francisco, CA, Citeseer, 1998, pp. 107–119.

[3] J. E. Rodgers, M. Çelebi, Seismic response and damage detection analyses of an instrumented steel moment-framed building, Journal of structural engineering 132 (10) (2006) 1543–1552.

[4] R. Chandramohan, L. M. Wotherspoon, B. A. Bradley, M. Nayyerloo, S. Uma, M. T. Stephens, Response of instrumented buildings under the 2016 Kaikoura earthquake., Bulletin of the New Zealand Society for Earthquake Engineering.

[5] F. Naeim, Learning from structural and nonstructural seismic performance of 20 extensively instrumented buildings, in: 12th World Conference on Earthquake Engineering, 2000.

[6] M. Çelebi, Current practice and guidelines for USGS instrumentation of buildings including federal buildings, in: Invited Workshop on Strong-Motion Instrumentation of Buildings, 2001, p. 21.

[7] S. Uma, A. King, J. Cousins, K. Gledhill, The GeoNet building instrumentation programme, Bulletin of the New Zealand Society for Earthquake Engineering 44 (1) (2011) 53.

[8] International Conference of Building Officials, Uniform Building Code, International Conference of Building Officials, 1997.

[9] FEMA, FEMA P-58-1: Seismic performance assessment of buildings. Volume 1–methodology, Federal Emergency Management Agency Washington, DC, 2012.

[10] E. Straser, A. Kiremidjian, T. Meng, L. Redlefsen, A modular, wireless network platform for monitoring structures, in: SPIE proceedings series, Society of Photo-Optical Instrumentation Engineers, 1998, pp. 450–456.

[11] J. P. Lynch, A. Sundararajan, K. H. Law, A. S. Kiremidjian, T. Kenny, E. Carryer, Embedment of structural monitoring algorithms in a wireless sensing unit, Structural Engineering and Mechanics 15 (3) (2003) 285–297.

[12] J. P. Lynch, A. Sundararajan, K. H. Law, A. S. Kiremidjian, E. Carryer, Embedding damage detection algorithms in a wireless sensing unit for operational power efficiency, Smart Materials and Structures 13 (4) (2004) 800.

[13] J. P. Lynch, K. H. Law, A. S. Kiremidjian, E. Carryer, C. R. Farrar, H. Sohn, D. W. Allen, B. Nadler, J. R. Wait, Design and performance validation of a wireless sensing unit for structural monitoring applications, Structural Engineering and Mechanics 17 (3-4) (2004) 393–408.

[14] J. P. Lynch, K. H. Law, A. S. Kiremidjian, J. E. Carryer, T. W. Kenny, A. Partridge, A. Sundararajan, Validation of a wireless modular monitoring system for structures, in: Smart Structures and Materials 2002: Smart Systems for Bridges, Structures, and Highways, Vol. 4696, International Society for Optics and Photonics, 2002, pp. 124–136.

[15] K. K. Nair, A. S. Kiremidjian, K. H. Law, Time series-based damage detection and localization algorithm with application to the ASCE benchmark structure, Journal of Sound and Vibration 291 (1) (2006) 349–368.

[16] H. Krawinkler, G. G. Deierlein, Challenges towards achieving earthquake resilience through performance-based earthquake engineering, in: Performance-based seismic engineering: Vision for an earthquake resilient society, Springer, 2014, pp. 3–23.

[17] S. Uma, Seismic instrumentation of buildings-a promising step for performance based design in New Zealand, in: NZSEE conference proceedings, 2007.

[18] K. Porter, J. Mitrani-Reiser, J. L. Beck, Near-real-time loss estimation for instrumented buildings, The Structural Design of Tall and Special Buildings 15 (1) (2006) 3–20.

[19] K. Porter, J. Mitrani-Reiser, J. L. Beck, J. Ching, Smarter structures: real-time loss estimation for instrumented buildings, in: Proceedings of the 8th US National Conference on Earthquake Engineering, Vol. 5, Curran Associates, 2006, pp. 2998–3007.

[20] S.-H. Hwang, D. G. Lignos, Nonmodel-based framework for rapid seismic risk and loss assessment of instrumented steel buildings, Engineering Structures 156 (2018) 417–432.

[21] S.-H. Hwang, D. Lignos, Proposed methodology for earthquake-induced loss assessment of instrumented steel frame buildings: building-specific and city-scale approaches, in: Proceedings of the 6th ECCOMAS Thematic Conference on Computational Methods in Structural Dynamics and Earthquake Engineering, no. CONF, 2017.

[22] M. Celebi, A. Sanli, M. Sinclair, S. Gallant, D. Radulescu, Real-time seismic monitoring needs of a building owner-and the solution: a cooperative effort, Earthquake Spectra 20 (2) (2004) 333–346.

[23] FEMA, NEHRP guidelines for the seismic rehabilitation of buildings, FEMA 273, prepared by the Applied Technology Council and the Building Seismic Safety Council for the Federal Emergency Management Agency Washington, DC, 1997.

[24] F. Naeim, S. Hagie, A. Alimoradi, E. Miranda, Automated post-earthquake damage assessment of instrumented buildings, Advances in Earthquake Engineering for Urban Risk Reduction (2006) 117–134.

[25] C. Rojahn, Procedures for postearthquake safety evaluation of buildings, ATC-20 Technical Report. Applied Technology Council (ATC) Redwood City, CA, 1989.

[26] J. Moehle, G. G. Deierlein, A framework methodology for performance-based earthquake engineering, in: 13th world conference on earthquake engineering, 2004, pp. 3812–3814.

[27] Haselton Baker Risk Group. Seismic Performance Prediction Program (SP3), `http://www.hbrisk.com` (2017).

[28] M. J. Huang, A. F. Shakal, Structure instrumentation in the California Strong Motion Instrumentation Program, in: Strong Motion Instrumentation for Civil Engineering Structures, Springer, 2001, pp. 17–31.

[29] M. P. Limongelli, Optimal location of sensors for reconstruction of seismic responses through spline function interpolation, Earthquake Engineering & Structural Dynamics 32 (7) (2003) 1055–1074.

[30] D. Hadjiharitou, Improving estimates of structural seismic motion, Master's thesis, Massachusetts Institute of Technology (2013).

[31] F. E. Udwadia, Methodology for optimum sensor locations for parameter identification in dynamic systems, Journal of Engineering Mechanics 120 (2) (1994) 368–390.

[32] P. Shah, F. Udwadia, A methodology for optimal sensor locations for identification of dynamic systems, ASME, Transactions, Journal of Applied Mechanics 45 (1978) 188–196.

[33] E. Heredia-Zavoni, L. Esteva, Optimal instrumentation of uncertain structural systems subject to earthquake ground motions, Earthquake engineering & structural dynamics 27 (4) (1998) 343–362.

[34] H. Guo, L. Zhang, L. Zhang, J. Zhou, Optimal placement of sensors for structural health monitoring using improved genetic algorithms, Smart Materials and Structures 13 (3) (2004) 528.

[35] F. Naeim, H. Lee, H. Bhatia, S. Hagie, K. Skliros, CSMIP instrumented building response analysis and 3-D visualization system (CSMIP-3DV), in: Proceedings of the SMIP-2004 Seminar, 2004.

[36] G. H. Behforooz, A comparison of the E(3) and not-a-knot cubic splines, Applied Mathematics and Computation 72 (2-3) (1995) 219–223.

[37] B. Efron, The jackknife, the bootstrap and other resampling plans, SIAM, 1982.

[38] M. Tomczak, Spatial interpolation and its uncertainty using automated anisotropic inverse distance weighting (IDW)-cross-validation/jackknife approach, Journal of Geographic Information and Decision Analysis 2 (2) (1998) 18–30.

[39] G. J. Bowen, J. Revenaugh, Interpolating the isotopic composition of modern meteoric precipitation, Water Resources Research 39 (10).

[40] M. D. Varljen, M. J. Barcelona, H. A. Wehrmann, A jackknife approach to examine uncertainty and temporal change in the spatial correlation of a VOC plume, Environmental Monitoring and Assessment 59 (1) (1999) 31–46.

[41] S. Smith, D. Holland, P. Longley, Quantifying interpolation errors in urban airborne laser scanning models, Geographical Analysis 37 (2) (2005) 200–224.

[42] D. L. Phillips, D. G. Marks, Spatial uncertainty analysis: propagation of interpolation errors in spatially distributed models, Ecological Modelling 91 (1-3) (1996) 213–229.

[43] H. Krawinkler, Van Nuys hotel building testbed report: exercising seismic performance assessment, PEER Report, 2005/11. Pacific Earthquake Engineering Research Center, College of Engineering, University of California, Berkeley, 2005.

[44] K. A. Porter, J. L. Beck, R. V. Shaikhutdinov, Investigation of sensitivity of building loss estimates to major uncertain variables for the Van Nuys testbed., PEER Report, 2002/0. Pacific Earthquake Engineering Research Center, College of Engineering, University of California, Berkeley, 2002.

[45] F. Naeim, Seismic performance of extensively instrumented buildings an interactive information system, CSMIP Report.

[46] B. S.-J. Chiou, R. R. Youngs, Update of the Chiou and Youngs NGA model for the average horizontal component of peak ground motion and response spectra, Earthquake Spectra 30 (3) (2014) 1117–1153.

[47] T. D. Ancheta, R. B. Darragh, J. P. Stewart, E. Seyhan, W. J. Silva, B. S.-J. Chiou, K. E. Wooddell, R. W. Graves, A. R. Kottke, D. M. Boore, et al., NGA-West2 database, Earthquake Spectra 30 (3) (2014) 989–1005.

[48] M. Baradaran Shoraka, Collapse assessment of concrete buildings: an application to non-ductile reinforced concrete moment frames, Ph.D. thesis, University of British Columbia (2013).

[49] E. Miranda, Approximate seismic lateral deformation demands in multistory buildings, Journal of Structural Engineering 125 (4) (1999) 417–425.

Appendix A. Building Information

Table A.2: Supplementary information for application buildings. The periods of the Van Nuys hotel are estimated using Table 2.4 of [43], which presents three approximations of the building's period calculated by different research teams. The periods of the residential building were estimated in [45], by analyzing instrumented records of the building for the Northridge earthquake.

Building Name	Van Nuys Hotel	Residential Building
CSMIP Station No.	24386	24601
Number of Stories	7	17
Design Year	1965	1980
Dimension [N-S] (ft)	63.00	226.67
Dimension [E-W] (ft)	151.00	79.75
Building Area (sf)	66591	307300
Period [N-S] (s)	1.5	0.8
Period [E-W] (s)	1.5	1.0
CSMIP Instrument Channel Nos. Used (N-S)	3, 4, 6, 8, 13, 14	5, 8, 10, 14
CSMIP Instrument Channel Nos. Used (E-W)	9, 10, 11, 12, 16	4, 7, 9, 12
Lateral System	Reinforced Concrete Interior Column-Slab Frames and Exterior Column-Spandrel Beam Frames	Precast Concrete Shear Wall
Lateral System Modeled in P-58 Analyses	Reinforced Concrete Perimeter Moment Frame	Reinforced Concrete Shear Wall

Appendix B. Ground Motion Prediction Equation

We used the [46] ground motion prediction equation (GMPE) for both application buildings. This GMPE predicts horizontal ground motion amplitudes caused by shallow crustal earthquakes, and is based on analysis of the NGA-West2 database [47] as well as numerical simulations. Parameter values used in the equation for both buildings are found in Table B.3.

Table B.3: GMPE parameter values for application buildings.

Building Name	Van Nuys Hotel	Residential Building
M	6.69	6.69
δ	40°	40°
λ	103°	103°
Z_{TOR} (km)	5	5
T (s)	1.5	0.9
R_{RUP} (km)	8.44	31.48
R_{JB} (km)	0	28.82
R_X (km)	7.18	13.73
$Z_{1.0}$ (km)	Unknown	Unknown
V_{S30} (m/s)	218.00	452.15
Δ_{DPP}	0	0
$F_{inferred}$	1	1
$F_{Measured}$	0	0
F_{RV}	1	1
F_{NM}	0	0
F_{HW}	1	0
Region	California	California

Appendix C. FEMA P-58 Simplified Analysis Method

The FEMA P-58 simplified analysis method [9] computes building EDPs using linear models, static analyses, and the lateral yield strength of the structure. It is important to note that this method contains a number of simplifying assumptions:

1. The method neglects vertical earthquake shaking, torsion, and soil-structure interaction effects.
2. The framing systems and responses are assumed to be independent along each horizontal axis of the building.
3. The method assumes that there are no significant discontinuities in strength and stiffness.
4. Story drift ratios cannot exceed 4%, and P-delta effects are ignored.
5. Story drift ratios are assumed to be less than four times the yield drift ratio, it is assumed that there is not excessive degradation in strength and stiffness, and bilinear elastic-plastic component behavior is assumed to be reasonable.
6. The method is calibrated for buildings less than 15 stories, and higher mode contributions are neglected.

Table C.4 provides parameter values used for both buildings in the method's equations (detailed in Section 5.3.1 of [9]). a and α are used to compute Δ_i in equation 5-10 of [9], using the equations for lateral displacement provided in [49].

Table C.4: FEMA P-58 simplified analysis parameter values for application buildings.

Building Name	Van Nuys Hotel	Residential Building
V_y	0.067	0.15
Δ_y	0.0075	0.0025
Soil Site Class	D	D
First Mode Mass Ratio	1.0	0.8
a	0.01	0.01
α	12.5	1.0